occurs in the understanding of the low intensity of the ground-state transition in P^{32}. Furthermore, the very weak intensities for the ground-state radiations in Si^{29} and Si^{30} are hard to reconcile with the single unit of angular momentum which must be radiated in these transitions if the spin of $\frac{1}{2}$ recently suggested for Si^{29} is correct.[4]

It is clear that the familiar selection rules concerning differences in parity and spin are not sufficient to account for the relative intensities of ground-state transitions. The experimental data, therefore, indicate the existence of additional parameters which determine the relative intensities of nuclear radiations. We wish to thank Dr. L. G. Elliott for helpful discussions.

[1] Kinsey, Bartholomew, and Walker, Phys. Rev. **77**, 723 (1950); **78**, 77 (1950).
[2] E. Feenberg and K. C. Hammack, Phys. Rev. **75**, 1877 (1949).
[3] F. B. Shull and E. Feenberg, Phys. Rev. **75**, 1768 (1949).
[4] Townes, Mays, and Dailey, Phys. Rev. **76**, 700 (1949).

The Viscosity of Liquid He^3

R. A. Buckingham
University College, London, England
AND
H. N. V. Temperley,
King's College, Cambridge, England
March 6, 1950

SOME recently announced results by Weinstock *et al.*[1] show that the viscosity of liquid He^3 increases smoothly from a value of 22 micropoise at 2.8°K to 30 micropoise at 1.05°K. The curve is everywhere convex to the temperature axis and shows no sign of a discontinuity anywhere in this range. Such a variation of viscosity is similar to that of an ordinary liquid, but it does not seem possible to explain it in the conventional way by assuming that the atoms moving through the liquid have potential barriers to surmount. Liquid He^4 (above the λ-point) already shows a viscosity increasing with temperature in much the same way as does that of a gas. The density of liquid He^3 is only just over half that of liquid He^4, and the effective height of any potential barrier is therefore correspondingly smaller. The fact that an opposite trend of viscosity is observed in liquid He^3 therefore points to an increase in mean free path as the temperature falls, which may be explained in one of two ways: (a) by a decrease in the effective cross-section at low velocities of impact of helium atoms (Ramsauer effect); (b) by a decrease in the effective cross section at low temperatures due to the scattered states being already occupied. The existence of such an effect in a Fermi gas was first pointed out by Tomonaga,[2] and a similar point has recently been made by Singwi and Kothari.[3]

We have examined the consequences of effect (a) alone, by extending to He^3 the calculations of the viscosity of He^4 gas made by Massey and Mohr,[4] and by Buckingham, Hamilton, and Massey.[5] Two models have been used, the rigid sphere model (with a diameter of 2.1A for a helium atom[4]), and another using an interaction potential formed from repulsive exponential and van der Waals attractive terms. This second potential is one called "potential C" by the second group of authors. Although the attractive part of potential C is too weak to represent the interaction of He atoms correctly, it happens that the adjustment to the correct magnitude is very nearly compensated by the smaller mass of He^3. Consequently the results of previous calculations are readily adapted to give values of viscosity which are probably a good approximation for He^3.

TABLE I. Theoretical values of η (in micropoise) as a function of T.

T (°K)	Rigid sphere ↑↓ (1)	Rigid sphere ↑↑ (2)	Rigid sphere Mixture (3)	Potential C ↓↑ (4)	Potential C ↑↑ (5)	Potential C Mixture (6)	Classical (7)	Complete degeneracy (8)	Observed (9)
0.25				3.6	5.3	4.7	3.6	—	
0.5	1.1	32	3.6	8.0	5.2	5.5	6.3	—	
0.75	1.6	19.5	4.7	6.0	4.8	5.0	8.7	41	
1.0	1.8	14.7	5.3	4.8	6.3	5.8	10.8	23	30.5
1.25	2.3	13.2	5.9	4.4	8.5	6.8	12.3	14.5	
1.5	2.7	12.2	6.4	4.4	11.0	8.0	13.5	10.2	
2.0	3.7	11.1	7.4	4.9	14.8	9.8	15.4	5.8	
2.5	4.7	10.8	8.2	5.7	15.9	11.0	17.0	3.8	22 at
3.0	5.8	11.0	9.0	6.7	15.4	11.6	18.5	2.5	2.80°K

In Table I, columns 1 and 2 refer to the rigid sphere model, and assume that the nuclear spins of each colliding pair of atoms are respectively antiparallel and parallel, whereas column 3 represents the consequences of assuming a 3:1 mixture of these two types of collision. Columns 4, 5, and 6 give corresponding results for the interaction potential C. Column 7 gives the viscosity of a classical gas of atoms of diameter 2.1A, while column 8 refers to the formula

$$\eta=(1/15\pi^3)\cdot(2mE_0{}^5)^{\frac{1}{2}}/(kT)^2\cdot(1/Q),$$

obtained by Tomonaga for an almost completely degenerate gas. (His actual expression refers to a mixture of two types of Fermi particle, so we have divided it by 2. The scattering cross section, Q, has been taken to be πr^2, r being taken as 1.05A, the gas-kinetic radius.) Since E_0, for the observed density (~0.07 g/cm³) of liquid He^3, corresponds to a Fermi degeneracy temperature of the order of 5°K, the Tomonaga formula is only the limiting form at very low temperatures.

Though it might seem that model 2 (rigid spheres with parallel spins) has at least the correct trend to interpret the observed results, it appears nervertheless that the Ramsauer effect is insufficient by itself to explain them: first, because model 5 shows that alteration of the interaction to a more correct form lowers the predicted viscosity at temperatures below 1.5°K considerably; secondly, because the effect of many-body collisions, neglected in models 1 to 7, can only shorten the mean free path; and thirdly, because models 2 and 5 seem to be practically ruled out by the observation of Sydoriak and Hammel[6] that liquid He^3 is not ferromagnetic within the range of temperatures considered.

We thus seem forced to conclude that the observed rise in viscosity as the temperature falls is due, at least in part, to the effect of the exclusion principle in reducing the probability of scattering.

[1] Weinstock, Osborne, and Abraham, conference on "Very Low Temperatures," Massachusetts Institute of Technology, 1949.
[2] S. Tomonaga, Zeits. f. Physik **110**, 573 (1938).
[3] K. S. Singwi and L. S. Kothari, Phys. Rev. **76**, 305 (1949).
[4] H. S. W. Massey and C. B. O. Mohr, Proc. Roy. Soc. **A141**, 434 (1934).
[5] Buckingham, Hamilton, and Massey, Proc. Roy. Soc. **A179**, 103 (1941).
[6] S. G. Sydoriak and E. F. Hammel, conference on "Very Low Temperatures," Massachusetts Institute of Technology, 1949.

The Nuclear Magnetic Moment of Praseodymium[141]

William H. Chambers, Robert E. Sheriff,* and Dudley Williams
Ohio State University, Columbus, Ohio
March 13, 1950

BY means of super-regenerative oscillator techniques similar to those previously described,[1,2] a nuclear magnetic resonance absorption peak for Pr^{141} has been located. By comparison of the resonance peak with the sodium resonance peak observed simultaneously in the same magnetic field, the following tentative value for the ratio of the resonance frequency of Pr^{141} to the resonance frequency of Na^{23} in sodium borate in the same applied field was obtained:

$$\nu(Pr^{141})/\nu(Na^{23})=1.2362\pm0.0006.$$

Using Pound's value for the ratio of the resonance frequency of Na^{23} to the resonance frequency of the proton in the same field,[3] one obtains the following value for the ratio of the resonance frequency of Pr^{141} to that of the proton:

$$\nu(Pr^{141})/\nu(H^1)=0.32698\pm0.00016.$$

On the basis of an interpolated value of 0.62 percent for the correction due to the diamagnetism of the atomic electrons as given by Lamb[4] for Hartree fields, and the value of the magnetic moment of the proton given by Mack,[5] the value of the nuclear g factor is:

$$g(\mathrm{Pr}^{141}) = 1.8375 \pm 0.0009.$$

The spin of praseodymium is known from hyperfine structure measurements[6] to be 5/2. Thus the magnetic moment is

$$\mu(\mathrm{Pr}^{141}) = 4.5938 \pm 0.0023 \text{ nuclear magnetons.}$$

The praseodymium resonance absorption was found in a saturated solution of praseodymium nitrate in water.

This value for the magnetic moment is in agreement with predictions made on the basis of Mayer's[7] theory of nuclear shell structure. According to this theory, praseodymium with 59 protons and 82 neutrons has one extra $4d$-proton in addition to the completed $5g$-proton sub-shell and $6h_{11/2}$ neutron shell. The calculated magnetic moment due to such a $4d$ proton is $+4.79$ nuclear magnetons. The sign of the magnetic moment cannot be determined from the present experimental results, but White's data[6] indicate definitely a positive value for the magnetic moment.[8]

We wish to express our appreciation to The Ohio State University Development Fund and Research Foundation for grants which made this work possible.

* AEC Fellow.

[1] J. R. Zimmerman and D. Williams, Phys. Rev. **76**, 350 (1949).
[2] W. H. Chambers and D. Williams, Phys. Rev. **76**, 638 (1949).
[3] R. V. Pound, Phys. Rev. **73**, 1112 (1948).
[4] W. E. Lamb, Jr., Phys. Rev. **60**, 817 (1941).
[5] J. W. Mack, Rev. Mod. Phys. **22**, 64 (1950).
[6] H. E. White, Phys. Rev. **34**, 1397 (1929).
[7] M. G. Mayer, Phys. Rev. **75**, 1969 (1949).
[8] Rosen, Harrison, and McNally, Phys. Rev. **60**, 722 (1941).

Cosmic-Ray Bursts in Ionization Chambers of Different Materials*

Harold W. Lewis
Department of Physics, Duke University, Durham, North Carolina
March 7, 1950

Measurements have been made of the cosmic-ray bursts in three cylindrical ionization chambers of different wall materials. The characteristics of the chambers and the burst sizes measured were such that nearly all the events were caused by nuclear disintegrations in the walls of the chambers.[1] Hence a comparison of the counting rates permits an approximate calculation of the relative cross sections for star production in the three materials, aluminum, copper, and lead.

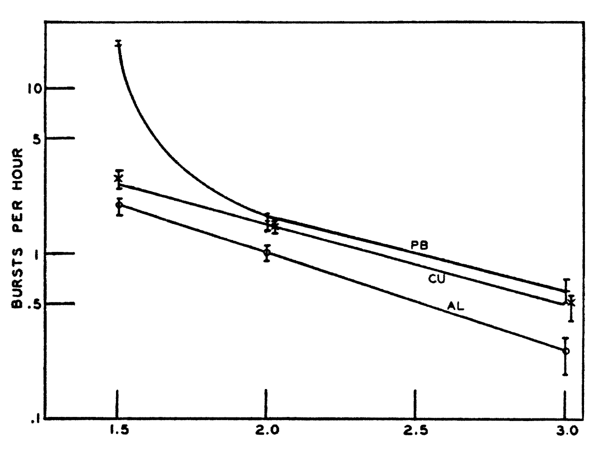

Fig. 1. Integral burst size distribution for three ionization chambers of different wall materials.

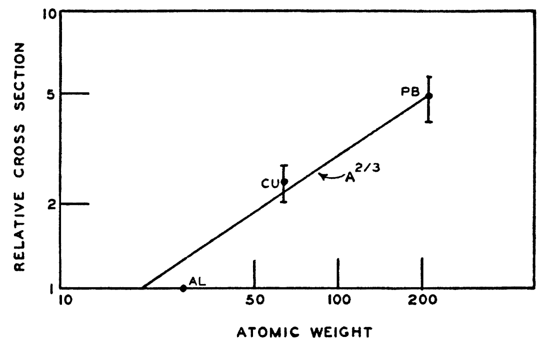

Fig. 2. Relative cross sections for star production calculated from ionization bursts larger than 2 Po-α.

The chambers were as nearly identical as possible, consisting of a cathode of $2\frac{1}{2}''$ outside diameter and $18''$ length, with a $0.030''$ collector wire. The wall thickness of the aluminum and copper chambers was $\frac{1}{16}''$ and of the lead $\frac{1}{8}''$. Because of the danger of porosity and the difficulty of soldering aluminum and lead, each chamber was enclosed in a larger brass case, the latter withstanding the high pressure. The case was 20 inches long and $3\frac{3}{4}''$ in diameter, with a $\frac{1}{16}''$ wall. The cathode was supported on insulators inside the case to permit the former to be operated at 1500 volts negative and the case and collector near ground. The active cylinder was equipped with end caps with clearance holes for the passage of the collector to Kovar glass seals on the ends of the case. Electron collection was used. Each chamber was filled with argon to a pressure of seven atmospheres and the gas purified by circulation through a hot calcium purifier. After purification, saturation occurred at about 1000 volts.

The pulse amplifiers were of the type designed by Jordan and Bell.[1] A rise time of 0.7 μsec. and RC clipping time of 40 μsec. were used. A multi-channel pulse height discriminator was used to obtain several points on an integral-bias curve simultaneously. Pulse shapes were not photographed. Calibration of the system was effected by a retractable polonium source rod mounted in the side of the chamber. The size of pulse produced by a polonium alpha-particle, corresponding to 5.3 Mev, is used as the unit for measuring burst size.

Measurements were made at Durham (elevation 400 feet) and on Mt. Mitchell (at an elevation of 6240 feet), the higher station giving four times the counting rate of the lower. Results obtained at Mt. Mitchell are shown in Fig. 1. Bursts smaller than 1.5 Po-α were not measured because of radioactive contamination of the chambers, nor above 3 Po-α because of the low counting rates at the altitudes used. An estimate of the number of bursts produced by electron showers was obtained by the use of a tray of counters directly below the chamber. The counter axes were perpendicular to the chamber axis, and alternate counters were connected in parallel, the two groups being connected in threefold coincidence with the chamber discriminator pulse. Bursts coincident with the discharge of at least one counter in each group indicated either a dense air shower or an event in the chamber itself in which two or more particles emerge and discharge counters. Such coincidences constituted 3 percent of the events in the aluminum and copper chambers and 15 percent of the events in lead. In the analysis below it is assumed that such coincidences are due to showers. The results in Fig. 1 represent the counting rates corrected for showers in this manner. The rapid rise in counting rate for lead below 2 Po-α is probably caused by long range contamination alpha-particles. The altitude variation in the bias curves, however, bears out the conclusion that the bursts above 2 Po-α are caused by nuclear disintegrations only.

The calculation of the relative star-production cross sections from the chamber counting rates can be only approximate, since the number of energy distribution of the nuclear fragments, protons and alpha-particles, is not known. The rough assumption